Current Research in Food Science 9 (2024) 100931

Contents lists available at ScienceDirect

Current Research in Food Science

journal homepage: www.sciencedirect.com/journal/current-research-in-food-science

Identification of novel antioxidant and anti-inflammatory peptides from bovine hemoglobin by computer simulation of enzymolysis, molecular docking and molecular dynamics

Xuan-Ying Xin [a], Chao-Hui Ruan [a], Yi-Hui Liu [a], Huai-Na Jin [a], Sung-Kwon Park [b], Sun-Jin Hur [c], Xiang-Zi Li [a,*], Seong-Ho Choi [d,**]

[a] Engineering Research Center of North-East Cold Region Beef Cattle Science & Technology Innovation, Ministry of Education, Department of Animal Science, Yanbian University, Yanji, 133002, China
[b] Department of Food Science and Biotechnology, Sejong University, Seoul, 05006, Republic of Korea
[c] Department of Animal Science and Technology, Chung-Ang University, Anseong, 17546, Republic of Korea
[d] Department of Animal Science, Chungbuk National University, Cheongju, 28644, Republic of Korea

ARTICLE INFO

Handling Editor: Dr. Yeonhwa Park

Keywords:
Bovine hemoglobin
Virtual enzymatic hydrolysis
Molecular docking
Molecular dynamics
Antioxidant peptide
Anti-inflammatory peptide
Keap1
TLR4

ABSTRACT

Due to the structural diversity and complex mechanisms of action of bioactive peptides, screening for specific functional peptides is often challenging. To efficiently screen bioactive peptides with antioxidant and anti-inflammatory effects from bovine hemoglobin, we employed bioinformatics methods to perform virtual enzymatic hydrolysis using online tools and predicted the bioactivity, toxicity, and sensitization scores of the resulting peptides. Molecular docking and molecular dynamics simulations with Keap1 and TLR4 were subsequently conducted to screen for antioxidant and anti-inflammatory peptides. Finally, peptides ARRF and ARNF were synthesized using the Fmoc solid-phase method. The oxidative stress and inflammation model in RAW264.7 cells was induced using lipopolysaccharide (LPS), followed by treatment with peptides ARRF and ARNF to verify their antioxidant and anti-inflammatory activities. The results demonstrated that 529 bovine hemoglobin oligopeptides were produced following virtual enzymatic hydrolysis, of which nine were identified as eligible based on predictions of biological activity, toxicity, solubility, and sensitization. Molecular docking results indicated that the oligopeptides ARNF, QADF, and ARRF exhibited favorable interactions with Keap1, while ARNF, RRF, and ARRF showed strong interactions with TLR4. The primary active sites binding to the Keap1 receptor included Val465, Thr560, and Gly464. The main active sites binding to the TLR4 receptor were Asn309, Asn305, and Glu286. Hydrogen bonding, electrostatic interactions, and hydrophobic interactions were identified as the primary modes of interaction between the oligopeptides and the Keap1 and TLR4 receptors. Molecular dynamics simulations further confirmed that the selected bovine hemoglobin peptides could stably bind to Keap1 and TLR4 receptors. Cell experiments demonstrated that ARRF and ARNF effectively ameliorated LPS-induced oxidative stress and inflammation in RAW264.7 cells.

Conclusion: Compared to traditional methods, this study promptly screens bovine hemoglobin antioxidant and anti-inflammatory peptides, offering a novel approach for rapidly identifying food-derived bioactive peptides.

1. Introduction

Bovine blood, a major by-product of cattle processing, is typically treated as waste, resulting in resource wastage. However, bovine blood is rich in nutrients such as protein, iron, and vitamins, making it a valuable resource (Aung et al., 2023). Previous research has shown that bovine blood can be utilized in various ways, such as extracting hemoglobin for the production of food additives and functional foods or preparing bioactive peptides for nutritional supplements and as raw materials for biomedical products (Hedhili et al., 2015). Mira et al. (Abou-Diab et al., 2020) applied bipolar membrane electrodialysis (EDBM) to hydrolyze hemoglobin, preparing bioactive peptides with

* Corresponding author.
** Corresponding author.
E-mail addresses: lxz@ybu.edu.cn (X.-Z. Li), seongho@cbnu.ac.kr (S.-H. Choi).

https://doi.org/10.1016/j.crfs.2024.100931
Received 4 September 2024; Received in revised form 3 November 2024; Accepted 17 November 2024
Available online 22 November 2024

antibacterial and antioxidant properties. Amer et al. (2022) demonstrated that bovine hemoglobin powder could serve as a protein source in the Nile tilapia diet, improving the fish's growth and immune status. Shaikhaliev et al. (2019) isolated bioactive peptide complexes from bovine serum and reported that these peptides could promote mesenchymal stromal cell proliferation and migration *in vitro* while accelerating bone defect healing in rats. Efficient utilization of bovine blood not only reduces processing by-product waste but also enhances economic benefits and promotes the sustainable use of resources.

Inflammation is a key factor in various diseases, including cardiovascular disease, diabetes, cancer, and neurodegenerative disorders, that pose serious risks to human health (Arulselvan et al., 2016). Current research emphasizes the development of anti-inflammatory drugs; however, anti-inflammatory peptides are considered a safer alternative to traditional drugs due to their high specificity and low toxicity (Biji et al., 2024). Gao et al. (2022) isolated and identified a bioactive peptide in bovine α-whey protein, which demonstrated anti-inflammatory and insulin resistance effects. Yan et al. (2013) hydrolyzed bovine lactoferrin to produce peptides, finding that these peptides exhibited potent anti-catabolic and anti-inflammatory biological activities in human joint tissues. Studies have shown that Toll-like receptor 4 (TLR4) is a central component of the mammalian innate immune system and plays a key role in bacterial endotoxin-mediated inflammation. TLR4 recognizes lipopolysaccharide (LPS) on the cell wall of Gram-negative bacteria, which subsequently activates the TLR4 signaling pathway, leading to the release of proinflammatory cytokines and chemokines and inducing an inflammatory response. TLR4 is the only TLR that activates both MyD88-and TRIF-dependent pathways. TLR4 initially recruits TIRAP at the cell membrane, which in turn facilitates MyD88 recruitment, triggering the activation of NF-κB and MAPK (Ciesielska et al., 2021; Płóciennikowska et al., 2015; Huang et al., 2021; Osman et al., 2024). Consequently, many studies have focused on designing compounds that regulate TLR4 expression, including antibodies, small molecule inhibitors, bioactive peptides, microRNAs, nanoparticles, lipid A analogues, and natural product derivatives, to achieve targeted anti-inflammatory effects.

Oxidative stress is a process in which free radicals are overproduced, damaging cells and leading to various diseases, including cancer, cardiovascular disease, and neurodegenerative disorders. Studies have shown that antioxidant peptides can neutralize free radicals and mitigate cellular and tissue damage induced by oxidative stress (Filomeni et al., 2015). Oxidative stress is closely linked to inflammation. When stimulated by lipopolysaccharide (LPS), the body produces a significant amount of free radicals, leading to the accumulation of reactive oxygen species (ROS) in mitochondria, which activates the NLRP3 inflammasome and promotes the release of interleukin (IL)-1β. Alternatively, it can activate the NF-κB signaling pathway, increasing the expression of interleukin-6 (IL-6), tumor necrosis factor α (TNF-α), inducible nitric oxide synthase (iNOS), cyclooxygenase-2 (COX-2), and nitric oxide (NO). Superoxide dismutase (SOD), an antioxidant enzyme, mitigates oxidative stress by scavenging reactive oxygen species (ROS). Malondialdehyde (MDA), a product of lipid peroxidation, reflects ROS levels, while glutathione (GSH) also participates in the antioxidant process, collectively maintaining redox balance. These molecules play a crucial role in the inflammatory process and significantly affect the overall health of the body (Sies and Jones, 2020; Ranneh et al., 2017). Ahlam et al. (Outman et al., 2023) enzymatically hydrolyzed bovine hemoglobin, resulting in bioactive peptides with antimicrobial and antioxidant activities. Wang et al. (2017) demonstrated that the bovine hemoglobin-derived peptide NFGK inhibits pancreatic cancer metastasis by targeting secreted Hsp90α and its downstream MMP-9. Studies have also shown that during oxidative stress, Keap1 undergoes conformational changes, leading to its dissociation from Nrf2. As a result, Nrf2 is no longer ubiquitinated and degraded, allowing it to translocate to the nucleus, where it exerts transcriptional activity and activates downstream pathways to play an antioxidant role. Therefore, Keap1 plays a critical negative regulatory role in the Nrf2/HO-1 anti-oxidative stress pathway (Bellezza et al., 2018; Yu and Xiao, 2021). Recent studies have demonstrated that bioactive peptides exhibit antioxidant and anti-inflammatory properties. However, because of the vast diversity of peptides and the traditional methods of peptide preparation, which typically involve using specific enzymes to digest proteins, followed by separation, identification, and activity confirmation through *in vitro* and *in vivo* experiments, screening bioactive peptides with specific functions remains relatively complex. With the advancement of bioinformatics, peptide databases, biological activity prediction tools, molecular docking, and molecular dynamics techniques have become increasingly prominent, allowing for protein enzymatic hydrolysis and activity prediction to be conducted through computer simulation experiments. Virtual enzymatic hydrolysis, based on the known restriction sites of various enzymes and amino acid sequences of target proteins, uses computer-aided methods to simulate the hydrolysis of protein peptide bonds by proteases, followed by the analysis of resulting small peptides and other products. Molecular docking and molecular dynamics simulations can rapidly screen for peptides with antioxidant and anti-inflammatory properties by simulating the docking of receptors and ligands, thereby elucidating the underlying mechanisms of action. This approach significantly enhances the efficiency of active peptide screening (Shuli et al., 2022).To address the issue of substantial bovine blood waste, a large number of antioxidant and anti-inflammatory peptides derived from bovine hemoglobin were rapidly screened. Candidate peptides were identified through virtual enzymatic digestion and biological activity prediction, and their interactions with TLR4 and Keap1 receptors were simulated using molecular docking and molecular dynamics to determine the most effective antioxidant and anti-inflammatory peptides. Finally, peptides ARRF and ARNF were synthesized using the Fmoc solid-phase method. The oxidative stress and inflammation model in RAW264.7 cells was induced using LPS, followed by treatment with peptides ARRF and ARNF to verify their antioxidant and anti-inflammatory activities. This approach offers a novel strategy for the development and reuse of bovine blood by-products generated during cattle processing.

2. Materials and methods

2.1. Materials, database and software

PBS buffer, DMEM high glucose medium, fetal bovine serum (FBS), and 0.25% trypsin EDTA were obtained from Gibco (San Diego, CA, USA). Lipopolysaccharide (LPS), and dimethyl sulfoxide (DMSO) were also acquired from Solaibao Technology Co., LTD. (Beijing, China). Kits for SOD, MDA, GSH-Px, and NO were sourced from the Nanjing Jiancheng Biological Engineering Research Institute (Nanjing, China). Elisa assay kits for IL-6, TNF-α, and IL-1βwere purchased from Shanghai Enzyme Linked Biotechnology Co., LTD. (Shanghai, China). CCK-8 and ROS kits were obtained from Shanghai Biyuntian Company (Shanghai, China). Total RNA extraction kit (adsorption column method), Beijing Tiangen Biochemical Technology Co., Ltd. (Beijing, China); first strand cDNA synthesis kit, Nanjing Novizan Biotechnology Co., Ltd. (Nanjing, China);

Database: UniProt database (https://www.uniprot.org/); BIOPEP (http://www.uwm.edu.pl/biochemia/index). Prot Param online tool (https://web.expasy.org/protparam/); ExPASy Peptide Cutter (http://web.expas.org/peptidecutter/) online tools; Peptide Ranker (http://bioware.ucd.ie/~compass/biowareweb/) online tool (Innovagenhttp://www.innovagen.com/proteomics-tools); online tools; ToxinPred (https://webs.iiitd.edu.in/raghava/toxinpred/index.html) online tools; AllerTOP Server Page (https://www.ddg-pharmfac.net/allertop/index.html) online system; INNOVAGEN online program (http://www.innovagen.com/proteomies-tools); The PDB database (http://www.rcsb.org/). Software: Pymol; AutoDock; Discovery Studio; Chemdraw; Chem3D; MOE 2019; Schordinger 2019

Table 1
Bovine hemoglobin chain.

Uniprot ID	Protein	Amino acid sequence	Amino acid number	Molecular weight/Da
P02070 ·	Hemoglobin subunit beta	MLTAEEKAAVTAFWGKVKVDEVGGEALGRLLVVYPWTQRFFESFGDLSTADAVMNNPKVKAHGKKVLDS FSNGMKHLDDLKGTFAALSELHCDKLHVDPENFKLLGNVLVVVLARNFGKEFTPVLQADFQKVVAGVANALAHRYH	145	15,954
P01966	Hemoglobin subunit alpha	MVLSAADKGNVKAAWGKVGGHAAEYGAEALERMFLSFPTTKTYFPHFDLSHGSAQVKGHGAKVAAALTKAVEHLD DLPGALSELSDLHAHKLRVDPVNFKLLSHSLLVTLASHLPSDFTPAVHASLDKFLANVSTVLTSKYR	142	15184
P02081	Hemoglobin fetal subunit beta	MLSAEEKAAVTSLFAKVKVDEVGGEALGRLLVVYPWTQRFFESFGDLSSADAILGNPKVKAHGKKVLDSFCEGLKQLD DLKGAFASLSELHCDKLHVDPENFRLLGNVLVVVLARRFGSEFSPELQASFQKVVTGVANALAHRYH	145	15859
A1A4Q3	Hemoglobin subunit mu	MLSAQERAHITQVWDLIAGHEAPFGAELLRRLFTVYPSTKVYFRHLGDHPDEVQLLSHGQRMLQAVGVAVQYMDNL RAVLSPLADLHAQVLRVDPTNFPLVIQCFQVVLASHLQGEFTVEMQAAWDKFLTGVAVVLTEKYR	141	15937
P06643	Hemoglobin subunit epsilon-4	MVHFTTEEKAAVASLWAKVNVEVVGGESLARLLIVYPWTQRFFDSFGNLYSESAIMGNPKVKAHGRKVLNSFGNAIE HMDDLKGTFADLSELHCDKLHVDPENFRLLGNMILIVLATHFSKEFTPQMQASWQKLTNAVANALAHKYH	147	16514
P06642	Hemoglobin subunit epsilon-2	MVHFTTEENVAVASLWAKVNVEVVGGESLARLLIVCPWTQRFFDSFGNLYSESAIMGNPKVKVYGRKVLNSFGNAIKH MDDLKGTFADLSELHCDKLHVDPENFRLLGNMILIVLATHFSKEFTPQMQAAWQKLTNAVANALTHKYH	147	16535

2.2. Selection of bovine hemoglobin-related protein sequences

A search using the validated amino acid sequence of bovine hemoglobin in the UniProt database identified six distinct protein chains (Table 1).

2.3. Computer simulation of proteolytic hydrolysis of bovine hemoglobin

Six bovine hemoglobin chains were virtually enzymatically digested using the ExPASy Peptide Cutter program, with three commonly used proteases, including trypsin (EC 3.4.21.4), pepsin (EC 3.4.23.1, pH 1.3, pH > 2), and papain (EC 3.4.22.2) (Minkiewicz et al., 2019).

2.4. Prediction of bioactivity, toxicity and physicochemical properties of bovine hemoglobin peptides

The PeptideRanker online tool was used to analyze the potential biological activity of peptides obtained after virtual enzymatic hydrolysis, selecting those with a bioactivity score greater than 0.5 as having potential biological activity (Mooney et al., 2012). ToxinPred was utilized to predict the potential toxicity of the peptides (Gupta et al., 2013). INNOVAGEN was employed to predict the water solubility and physicochemical properties of the peptides. Sensitization was assessed using the A11erTOP online software (Maurer-Stroh et al., 2019). Consequently, hemoglobin peptides with non-toxicity, favorable solubility, non-sensitization, and high biological activity were identified.

2.5. Molecular docking of bovine hemoglobin peptides to TLR4 and Keap1 receptors

The 3D structures of the oligopeptides were constructed using ChemDraw and Chem3D. The RCSB PDB database was used to retrieve the TLR4 and Keap1 structures as molecular docking receptors. PyMOL software was utilized to remove water molecules and phosphate groups from the proteins and save them as PDB files. The Molecular Operating Environment (MOE) 2019 software was employed to perform energy minimization on the peptides, pretreat the TLR4 (PDB ID: 2Z63) and Keap1 (PDB ID: 2FLU) receptors, and identify active pockets. Finally, MOE 2019 was employed for molecular docking. The binding affinities were assessed based on binding energy, and the results were visualized using PyMOL software.

2.6. Molecular dynamics simulation of bovine hemoglobin peptides with TLR4 and Keap1 receptors

The operation was conducted using the Schrödinger 2019 software "Desmond" module. A predefined SPC water model was employed to simulate water molecules within the OPLS2005 force field. To neutralize the system, an appropriate amount of chloride or sodium ions was added and randomly distributed within the solvation system. After constructing the solvation system, energy minimization was performed with the default protocol integrated into the Desmond module, applying OPLS2005 force field parameters. Nose-Hoover temperature coupling and isotropic scaling were utilized to maintain the temperature at 300 K and pressure at 1 atm. Following this setup, 50 ns of NPT simulations were run, with trajectories saved at 50 ps intervals.

2.7. Solid phase synthesis of polypeptides

Polypeptide was synthesized by solid phase synthesis. The condensation and removal reactions were conducted alternately, beginning with the first amino acid at the C-terminal of the selected active peptide sequence, progressing to the N-terminal, until all remaining amino acids were condensed onto the resin. The reaction was verified using the ninhydrin method. The resin was separated from the polypeptide using a lysate, resulting in the acquisition of the crude peptide following repeated washing with ice ether and subsequent filtration. The molecular weight of the crude product was determined using mass spectrometry, followed by purification through high-performance liquid chromatography and lyophilization, yielding a purified polypeptide.

2.8. Cell experimental study

2.8.1. Cell culture

The recovered RAW264.7 cells were transferred into sterile culture flasks, and a high-glucose DMEM medium supplemented with 10% fetal bovine serum and 1% antibiotics (streptomycin and penicillin) was added. The cells were incubated at 37 °C with 5% CO_2, and the culture medium was regularly replaced.

2.8.2. The effect of peptides ARRF and ARNF on RAW264.7 cell viability was detected by CCK-8 method

After the cells reached the logarithmic growth phase, 100 μL of the uniform cell suspension was added to each well of a 96-well plate; the density was 3000 cells per well, and the surrounding wells were sealed with PBS and incubated for 24 h. After adding 0, 0.1, 0.3, 0.5, 0.7, 1.0, and 1.5 mg/mL peptides ARRF and ARNF solution for 24 h, the culture medium was aspirated and the wells were washed twice with PBS. The CCK-8 solution was prepared by diluting it with a complete medium. 100 μL of CCK-8 solution was added to each well, and cell viability was assessed after incubating for 3 h. Absorbance values were measured at a wavelength of 450 nm.

2.8.3. LPS-induced inflammation in RAW264.7 cells and experimental grouping

RAW264.7 cells (1.5×10^4 cells per well) were seeded in six-well plates and incubated for 24 h. Except for the blank group, all other groups were treated with 1 μg/mL LPS for 24 h. Following treatment, the

Table 2
Oligopeptides with potential biological activity.

Peptide sequence	Bioactivity score	Peptide sequence	Bioactivity score
ML	0.894564	PA	0.53447
WG	0.992384	LR	0.569984
RL	0.626352	YR	0.525242
RF	0.986556	MF	0.996643
SF	0.948796	YF	0.981812
AF	0.973259	CF	0.99641
NF	0.941145	WD	0.917723
AG	0.546994	PL	0.811148
RM	0.847822	WA	0.957038
PG	0.877086	HF	0.950971
IM	0.696975	HM	0.677981
QM	0.607122	AW	0.9669
WQ	0.909891	GRL	0.775024
GDL	0.546664	DSF	0.725605
PWT	0.892829	ADF	0.806246
PHF	0.938016	DKF	0.660518
AWG	0.949222	RRF	0.939558
ASF	0.772311	QCF	0.968685
SPL	0.665423	RRL	0.584042
SWQ	0.698752	NSF	0.686594
VHF	0.555798	GNL	0.549969
ARL	0.522998	KGTF	0.620703
ARNF	0.767797	QADF	0.638734
NFGK	0.609045	ERMF	0.776511
PGAL	0.71419	PSDF	0.818593
ARRF	0.877805	KGAF	0.746432
QASF	0.574244	GSEF	0.542479
VYFR	0.66379	QGEF	0.627572
MVHF	0.742263	AIMG	0.643562
NMIL	0.575237	ATHF	0.556806
AAWGK	0.661786	AWDKF	0.916117
GNMIL	0.677182	VCPWT	0.824502
IVCPWT	0.697057	IVYPWT	0.599219
QYMDNL	0.589466	VVYPWT	0.502875
SNGMKHL	0.567183	SHGQRML	0.603457

cells were incubated with peptides ARRF and ARNF at a concentration of 0.7 mg/mL for 24 h.

2.8.4. Determination of the contents of NO, TNF-α, IL-6, and PGE_2

The cells were incubated as previously described. Following cell culture, the supernatant was collected and centrifuged to remove residual cells. The corresponding contents were quantified by the instructions of the NO content detection kit and the ELISA kit for TNF-α, IL-6, and PGE_2 detection.

2.8.5. Determination of ROS content, SOD, MDA, and GSH-Px levels

The cells were incubated as described above. According to the ROS kit instructions, the DCFH-DA fluorescent probe method was used to detect ROS levels, using fluorescence microscope images and ImageJ software for semi-quantitative analysis of fluorescence intensity. The levels of SOD, MDA, and GSH-Px in the cells were measured according to the kit instructions.

2.8.6. Statistical analyses

For the simulated data, the simulated results were determined three times in this study to reduce the influence of random errors. All test data are presented as the mean ± standard deviation from three experiments (mean ± SD, n = 3). One-way analysis of variance was performed using GraphPad Prism 8.02 software to compare the data. p-values of <0.01 and < 0.05 were considered indicative of significant differences between groups.

3. Results

3.1. Computer simulation of proteolytic hydrolysis of bovine hemoglobin

Six bovine hemoglobin chains were digested with trypsin (EC3.4.21.4), pepsin (pH1.3, pH > 2, EC3.4.23.1), and papain (EC3.4.22.2), respectively. A total of 529 oligopeptides were obtained.

Table 3
Evaluates the water solubility, toxicity, and allergenicity of bovine hemoglobin peptides.

Peptide sequence	Bioactivity score	Water solubility	Toxicity	Allergenicity
DSF	0.725605	Easily soluble in water	Nontoxicity	No allergenicity
KGTF	0.620703	Easily soluble in water	Nontoxicity	No allergenicity
ARNF	0.767797	Easily soluble in water	Nontoxicity	No allergenicity
QADF	0.638734	Easily soluble in water	Nontoxicity	No allergenicity
DKF	0.660518	Easily soluble in water	Nontoxicity	No allergenicity
ERMF	0.776511	Easily soluble in water	Nontoxicity	No allergenicity
RRF	0.939558	Easily soluble in water	Nontoxicity	No allergenicity
ARRF	0.877805	Easily soluble in water	Nontoxicity	No allergenicity
VYFR	0.66379	Easily soluble in water	Nontoxicity	No allergenicity

3.2. Evaluation of bioactivity of bovine hemoglobin peptide

These 529 peptides were evaluated using the PeptideRanker online tool, and a total of 70 peptides with potential activity (score ≥0.5) were identified (Table 2). The selected peptides include 25 dipeptides, 18 tripeptides, 17 tetrapeptides, 4 pentapeptides, 4 hexapeptides, and 2 heptapeptides.

3.3. Evaluation of water solubility, toxicity and sensitization of bovine hemoglobin peptide

The water solubility, toxicity, and sensitization of the screened oligopeptides with potential biological activity were predicted, resulting in the identification of 9 good water-soluble, non-toxic, and non-allergenic oligopeptides (Table 3). The molecular formulas of these oligopeptides are depicted in Fig. 1.

3.4. Molecular docking results of bovine hemoglobin peptide with TLR4 and Keap1 receptors

The interactions of the nine oligopeptides with the Keap1 and TLR4 receptors are illustrated in Figs. 2 and 3. According to the docking results, all nine oligopeptides were able to penetrate the binding pockets of Keap1 and TLR4, respectively. The docking energies of the oligopeptides with the Keap1 receptor ranged from −8.3393 to −9.4007 kcal/mol, with an average of −8.8994 kcal/mol. For the TLR4 receptor, the energies ranged from −6.7031 to −7.7272 kcal/mol, with an average of −7.0472 kcal/mol. The stability of the receptor-ligand complex can be assessed by the docking binding energies, with lower energies indicating more stable complexes (Gupta et al., 2013). Further analysis identified the primary active sites for oligopeptide binding to the Keap1 receptor as Val465, Thr560, Gly464, Val604, and Gly605, with Val465 being the most frequently bound, followed by Gly605, Thr560, and Val604. For the TLR4 receptor, the main active sites were Asn309, Asn305, Glu286, Cys281, Glu254, and Leu283, with Asn309 being the most frequently observed at the docking site. Hydrogen bonding was the predominant interaction mode between the oligopeptides and the Keap1 and TLR4 receptors. Additionally, electrostatic and hydrophobic interactions were also present.

The binding energies of ARNF, QADF, and ARRF to the Keap1 receptor were relatively low, indicating that these three oligopeptides

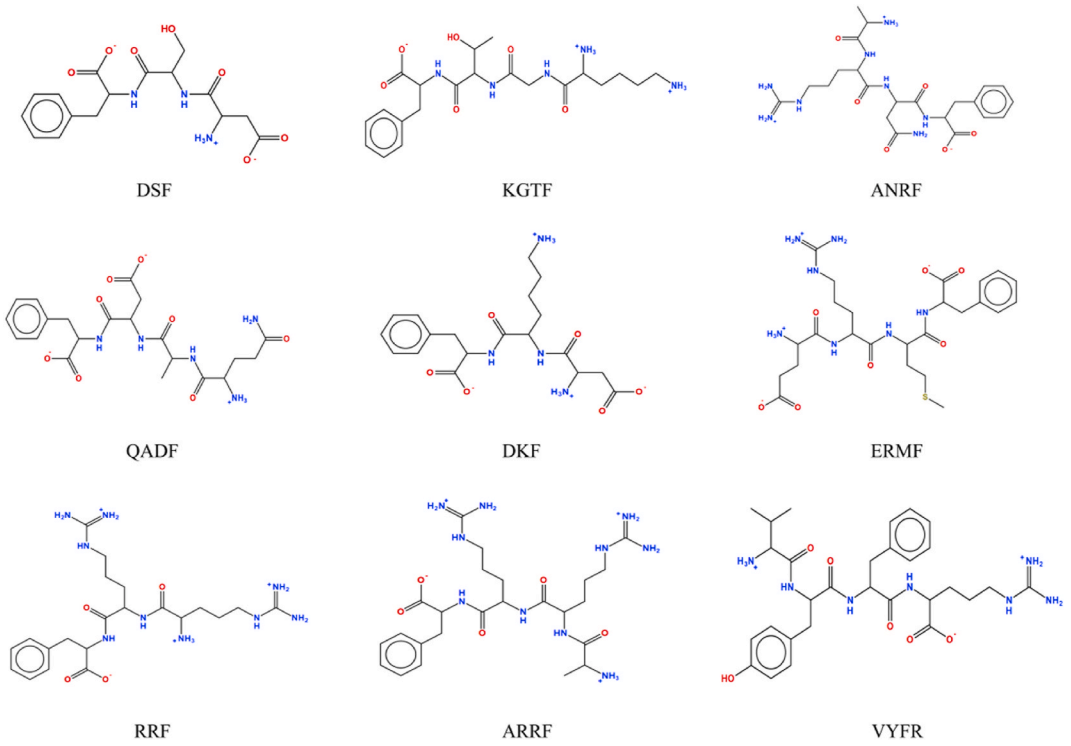

Fig. 1. Molecular formula of oligopeptide.

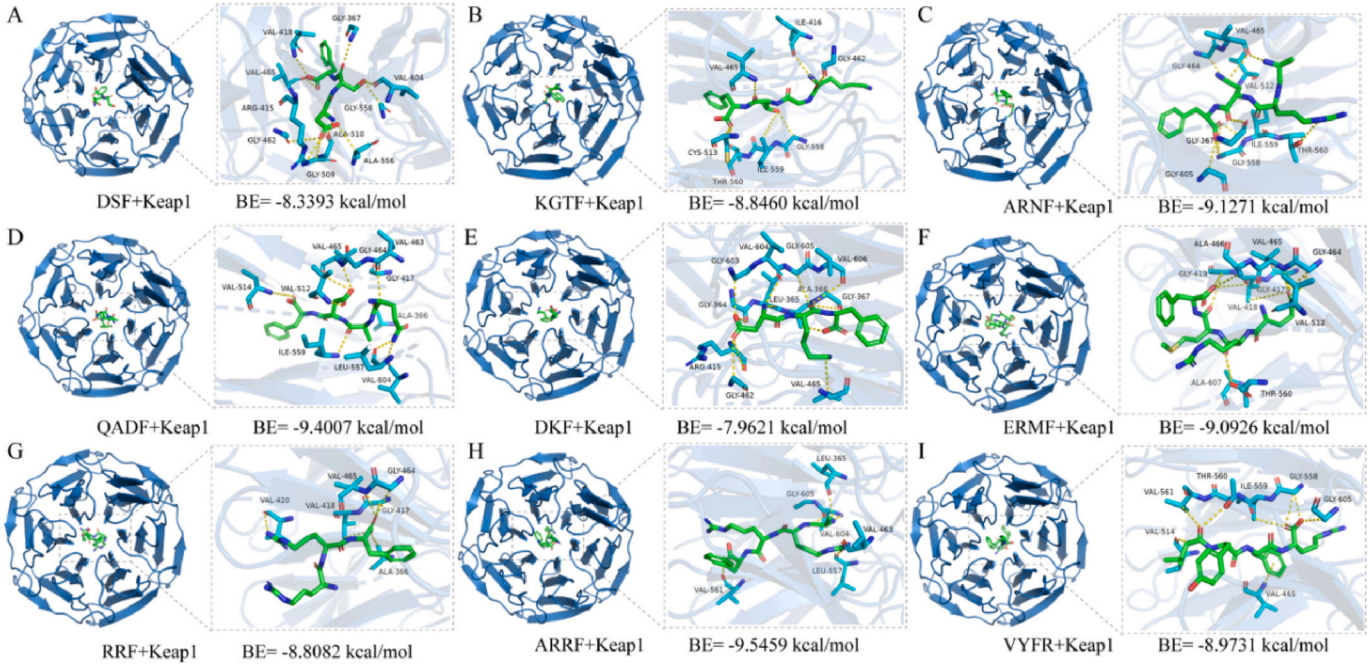

Fig. 2. Molecular docking results between hemoglobin peptide and Keap1 receptor.

exhibit stronger antioxidant capacity. Among them, ARRF, with the lowest binding energy (−9.5459 kcal/mol), interacted with the Keap1 receptor and was able to form hydrogen bonds with multiple binding sites (Val604, Leu557, Val463, Gly605, Val561). Leu557, Val604, Ala366, Gly417, Ile559, Val512, Gly464, Val465, and Val514 of Keap1 formed hydrogen bonds with QADF during the binding process. The oligopeptide ARNF also formed hydrogen bonds with multiple amino acid residues (Thr560, Gly367, Gly464, Val465, Val512, Ile559, Gly558, Gly605) in Keap1. When bound to the TLR4 receptor, ARRF exhibited the lowest binding energy (−7.7272 kcal/mol). Glu254, Cys306, Leu283, Glu286, and Ser311 in the TLR4 receptor form hydrogen bonds with ARRF, and Glu254 also forms an ionic interaction with this oligopeptide. The peptide ARNF also exhibited a lower binding energy (−7.5779 kcal/mol). As shown in Fig. 3, ARNF forms hydrogen bond interactions with Glu254, His256, Glu286, and Asn309 residues of the TLR4 receptor. Glu254 forms an ionic bond with ARNF, and Asn309

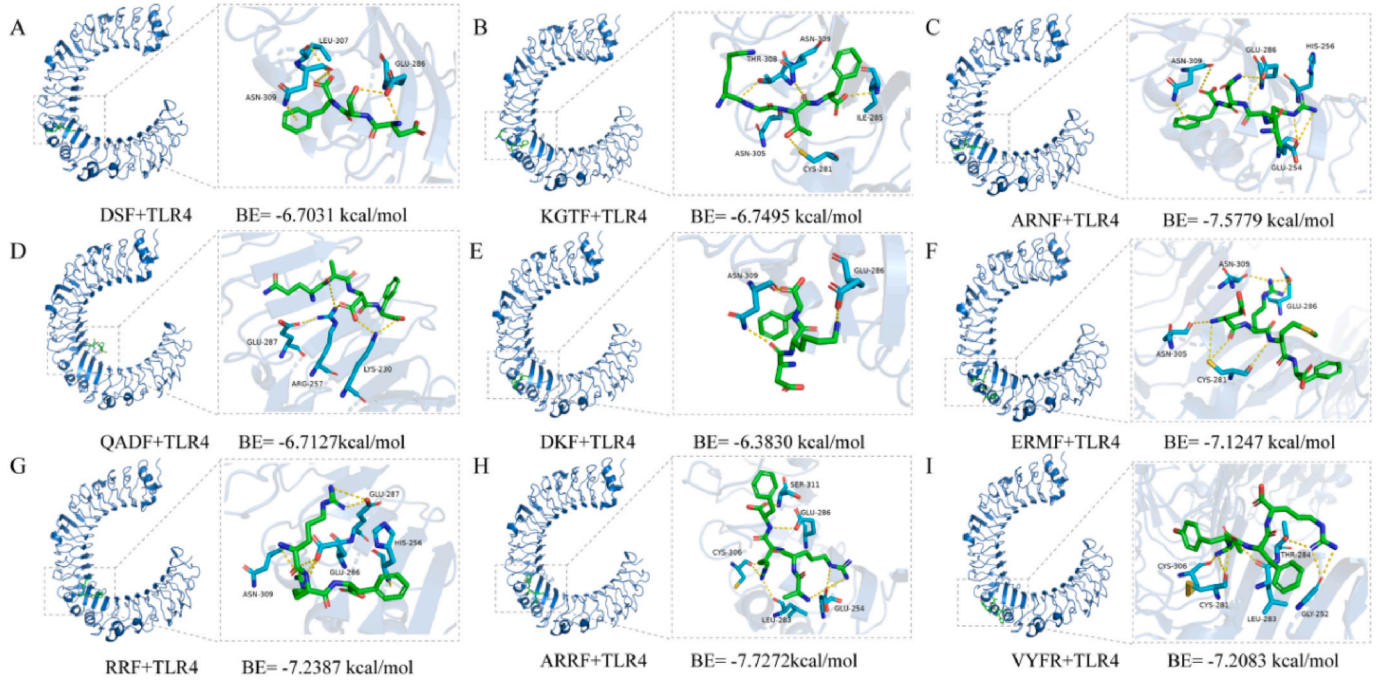

Fig. 3. Molecular docking results between hemoglobin peptide and TLR4 receptor.

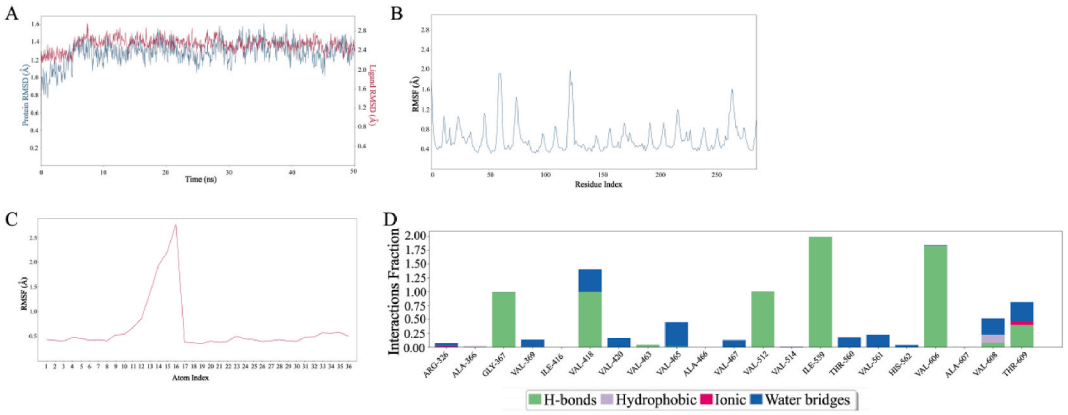

Fig. 4. Molecular dynamics simulation analysis of docking results between ARNF and Keap1 protein. (A) Root mean square deviation (RMSD), (B–C) root mean square fluctuation (RMSF), and (D) type of interaction between ARNF and Keap1 during the simulation.

forms a hydrophobic interaction with ARNF. RRF primarily interacts with the TLR4 receptor through hydrogen bonds, including Glu287, Glu286, and Asn309. Glu287 and Glu286 in the TLR4 receptor form ionic bonds with the ligand RRF. In addition, RRF forms a hydrophobic interaction with His256 in the TLR4 receptor. Therefore, ARNF, QADF, and ARRF exhibit stronger antioxidant capacities than other oligopeptides. ARRF, ARNF, and RRF exhibit stronger anti-inflammatory abilities.

3.5. Molecular dynamics simulation results of bovine hemoglobin peptide and TLR4 and Keap1 receptors

Given the favorable docking of oligopeptides ARNF, QADF, and ARRF with Keap1, and ARNF, RRF, and ARRF with TLR4, these oligopeptides were selected for molecular dynamics simulations over 50 ns to further evaluate their interactions with Keap1 and TLR4. Figs. 4–9 present the results of the molecular dynamics simulations. The root mean square deviation (RMSD) was used as the criterion to evaluate the stability of the binding systems of the active peptides with Keap1 and TLR4 receptors. The complexes of these bioactive peptides with Keap1 and TLR4 receptors reached equilibrium after 10 ns and 30 ns, respectively. The average RMSD values for QADF/Keap1 and RRF/TLR4 were 1.08 Å and 2.36 Å, respectively, which were lower than those of other complexes, indicating that the QADF/Keap1 and RRF/TLR4 complexes may exhibit higher stability. The root mean square fluctuation (RMSF) quantifies the fluctuation of each atom relative to its average position, reflecting the flexibility of each protein region. Therefore, RMSF values were calculated for the entire 50 ns simulation. The RMSF of all six peptides was low, with most regions on the Keap1 receptor below 1.2 Å and most regions on TLR4 below 2 Å, indicating that these two protein systems are relatively stable. The Keap1 protein system was more stable than the TLR4 system, which is consistent with the docking results. Similarly, the QADF/Keap1 and RRF/TLR4 complexes exhibited lower RMSF values. Protein-ligand interactions were monitored throughout the simulation. These interactions were categorized and summarized by type, as shown in the figure. Protein-ligand interactions (or "contacts")

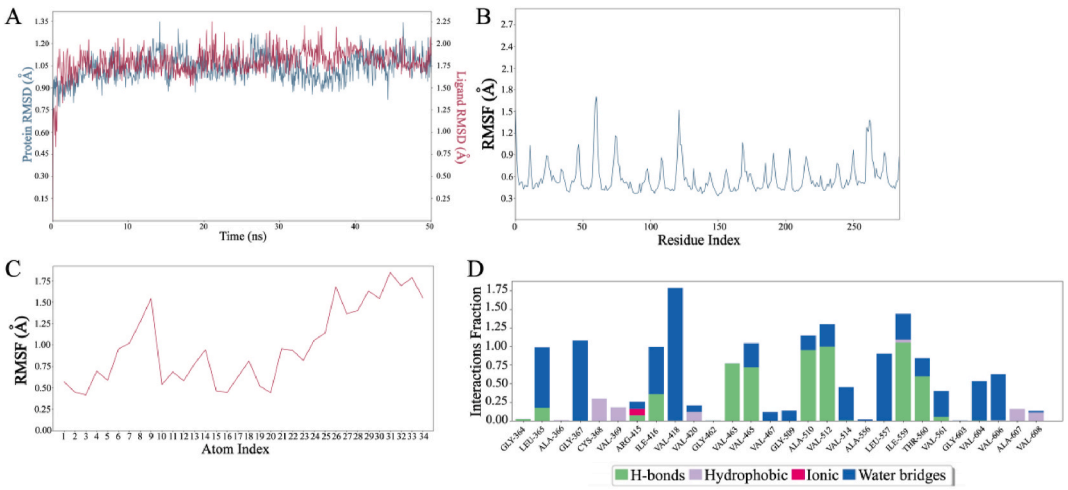

Fig. 5. Molecular dynamics simulation analysis of QADF docking results with Keap1 protein. (A) Root mean square deviation (RMSD), (B–C) root mean square fluctuation (RMSF), and (D) type of interaction between QADF and Keap1 during the simulation.

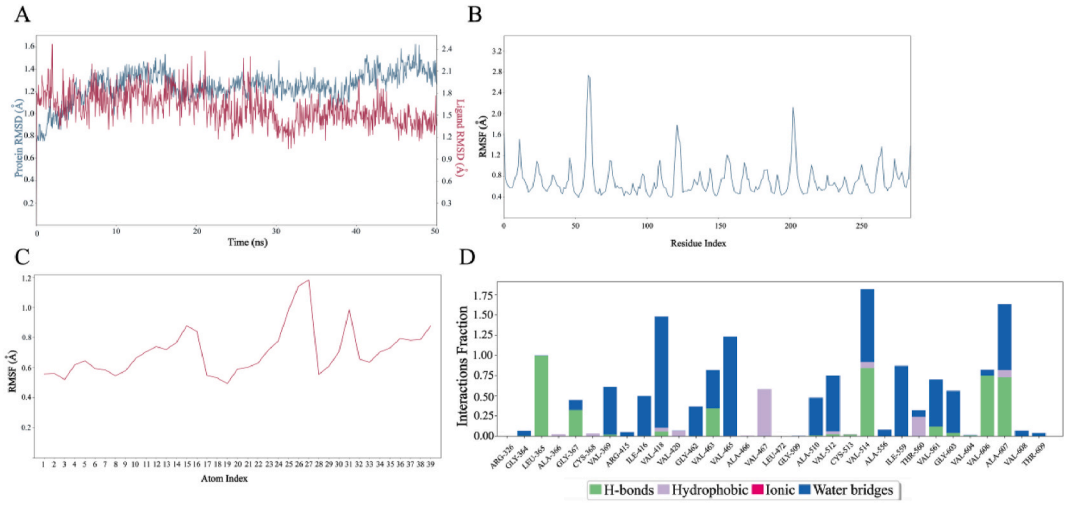

Fig. 6. Molecular dynamics simulation analysis of docking results between ARRF and Keap1 protein. (A) Root mean square deviation (RMSD), (B–C) root mean square fluctuation (RMSF), and (D) type of interaction between ARRF and Keap1 during the simulation.

were classified into four types: hydrogen bonds (green), hydrophobic interactions (light pink), ionic bonds (red), and water bridges (blue). There were more hydrogen bonds and water bridges in the interactions between these oligopeptides and Keap1 and TLR4.

The RMSD results for ARNF and Keap1 are presented in Fig. 4A. The figure indicates that the RMSD of the receptor protein is below 1.6 Å, while the RMSD of the ligand ARNF ranges from 2.4 Å to 2.8 Å throughout the simulation, suggesting that the protein remains stable relative to the ligand. The RMSF of the ligands ranged from 0.5 Å to 2.7 Å (Fig. 4C), and the RMSF results for the Keap1 protein with ARNF are presented in Fig. 4B; the total RMSF value of the protein remained below 2.8 Å. The bar graph illustrating Keap1 protein interactions with ARNF indicates a higher number of hydrogen bond interactions during the simulation (Fig. 4D). During the simulation of Keap1 and ARNF, Gly367, Val418, Val512, Ile559, Val606, and Thr609 exhibited hydrogen bond interactions, while Val608 exhibited hydrophobic interactions.

Throughout the simulation of QADF and Keap1, the RMSD of the protein was generally below 1.2 Å, while the RMSD of the ligand QADF ranged from 1.5 to 2.0 Å. The RMSF of the ligand ranges from 0.4 Å to 1.8 Å (Fig. 5C), and the RMSF results for the Keap1 protein with QADF are presented in Fig. 5B, with the total RMSF value of the protein remaining below 1.8 Å. The bar graph illustrating the interactions between Keap1 protein and ARNF indicates a higher number of hydrogen bond interactions during the simulation (Fig. 5D). During the simulation of Keap1 and QADF, Ile559, Val512, and Val465 were critical in forming hydrogen bonds with QADF, while Cys368, Val369, Val420, Ala607, and Val608 exhibited hydrophobic interactions. Additionally, Arg415 exhibited ionic interactions during the binding process with QADF.

Throughout the simulation of ARRF and Keap1, the protein RMSD ranged from 0.8 to 1.6 Å, while the RMSD of the ligand ARRF ranged from 1.2 to 1.6 Å (Fig. 6A). The RMSF of the ligand ranged from 0.5 to 1.2 Å (Fig. 6C), and the RMSF results for the Keap1 receptor with ARRF are presented in Fig. 6B, with the total RMSF value of the protein below 2.8 Å, indicating greater stability between residues 125 and 200. The Keap1 receptor and ARRF exhibited stronger interaction forces during the simulation (Fig. 6D). During the simulation of Keap1 and ARRF, Leu365, Gly367, Val463, Val514, Val606, and Ala607 were critical in forming hydrogen bonds with ARRF, while Val467 and Thr560 exhibited hydrophobic interactions.

Throughout the simulation of ARNF and TLR4, the RMSD values for both the protein and the ligand were relatively unstable. The RMSD of the protein ranged from 1.0 to 4.0 Å, while that of the ARNF ligand

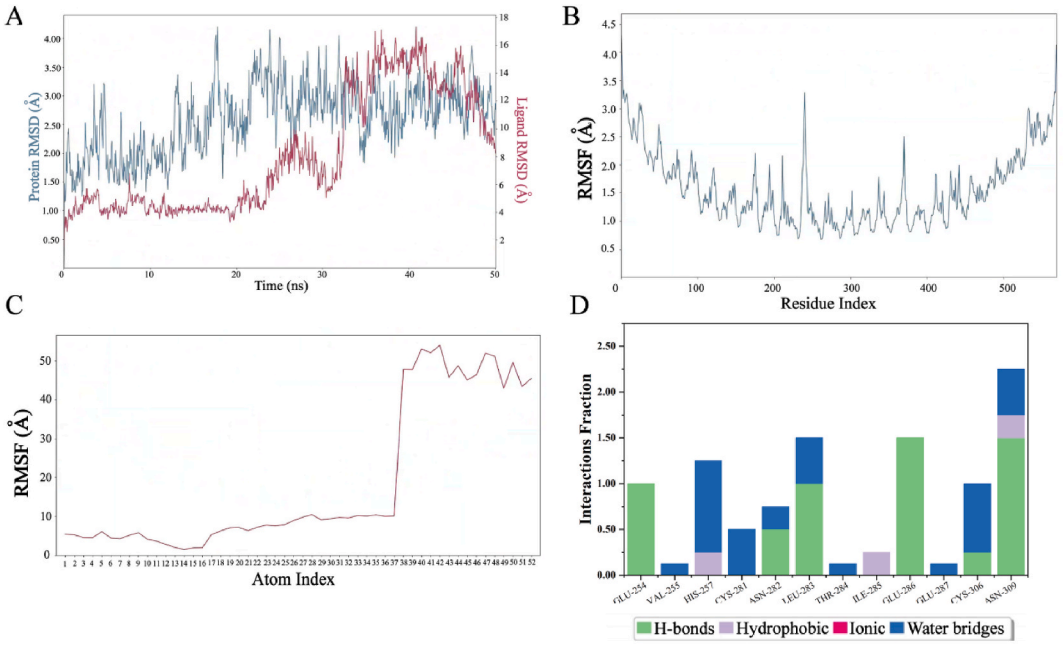

Fig. 7. Molecular dynamics simulation analysis of docking results between ARNF and TLR4 protein. (A) Root mean square deviation (RMSD), (B–C) root mean square fluctuation (RMSF), and (D) type of interaction between ARNF and TLR4 during the simulation.

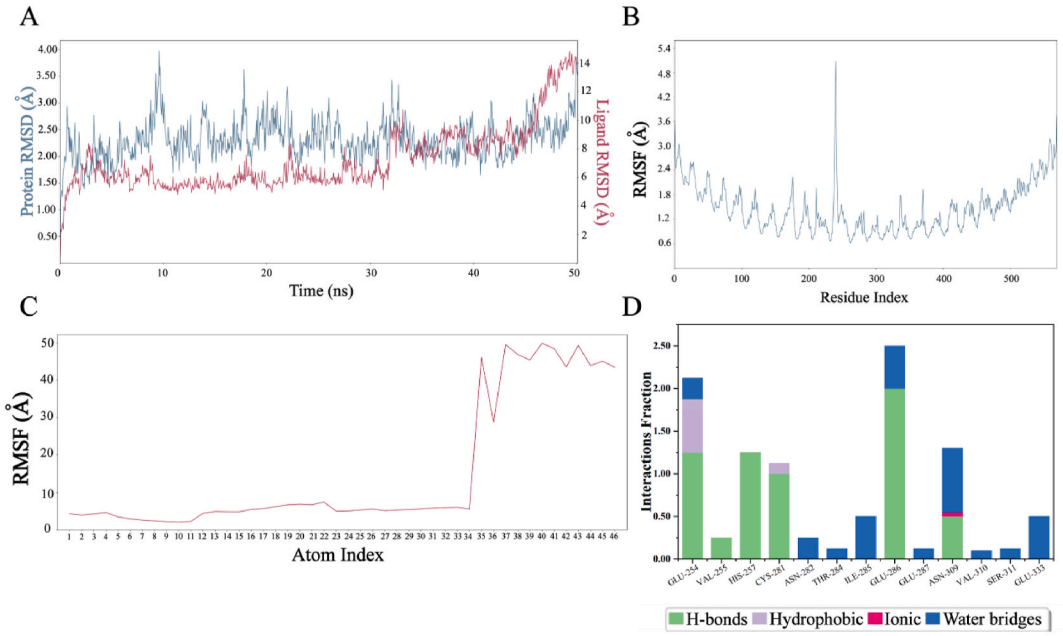

Fig. 8. Molecular dynamics simulation analysis of docking results between RRF and TLR4 protein. (A) Root mean square deviation (RMSD), (B–C) root mean square fluctuation (RMSF), and (D) type of interaction between RRF and TLR4 during the simulation.

ranged from 4.0 to 16.0 Å (Fig. 7A). The RMSF of the ligand ranged from 3.0 to 55.0 Å (Fig. 7C), and the RMSF results for the TLR4 protein with ARNF are presented in Fig. 7B, with the total RMSF value of the protein being less than 3.5 Å, indicating greater stability between residues 250 and 380. The interaction forces between TLR4 and ARNF were weaker than those between Keap1 and ARNF during the simulation (Fig. 7D). During the simulation of TLR4 and ARNF, Glu254, Asn282, Leu283, Glu286, Cys306, and Asn309 were critical in forming hydrogen bonds with ARNF, while His257, Ile285, and Asn309 exhibited hydrophobic interactions.

Throughout the simulation of RRF and TLR4, the protein RMSD ranged from 1.5 to 3.8 Å, while the RMSD of the RRF ligand was between 2.0 and 14.0 Å (Fig. 8A). The RMSF of the ligand ranged from 3.0 to 48.0 Å (Fig. 8C), and the RMSF results for the TLR4 protein with RRF are presented in Fig. 8B, with the total RMSF values for the protein below 5.0 Å, indicating greater stability between residues 280 and 380. During the simulation of TLR4 and RRF, Glu254, Val255, His257, Cys281, Glu286, and Asn309 were critical in forming hydrogen bonds with RRF. Glu254 and Cys281 exhibited hydrophobic interactions during the simulation. Residue Asn309 also displayed ionic interactions (Fig. 8D).

Throughout the simulation of ARRF and TLR4, the protein RMSD ranged from 1.5 to 4.3 Å, while the RMSD of the ARRF ligand was

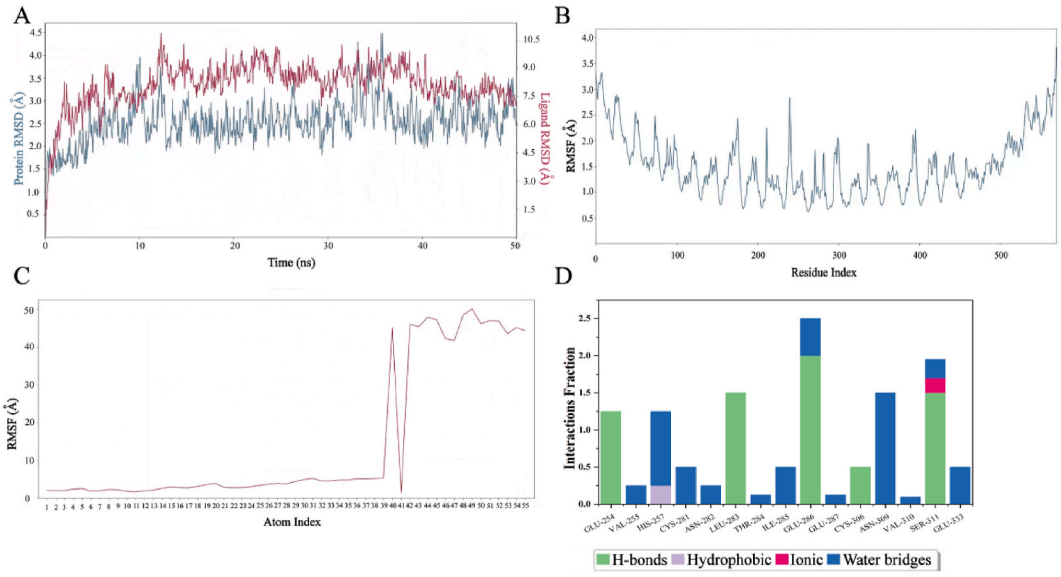

Fig. 9. Molecular dynamics simulation analysis of docking results between ARRF and TLR4 protein. (A) Root mean square deviation (RMSD), (B–C) root mean square fluctuation (RMSF), and (D) type of interaction between ARRF and TLR4 during the simulation.

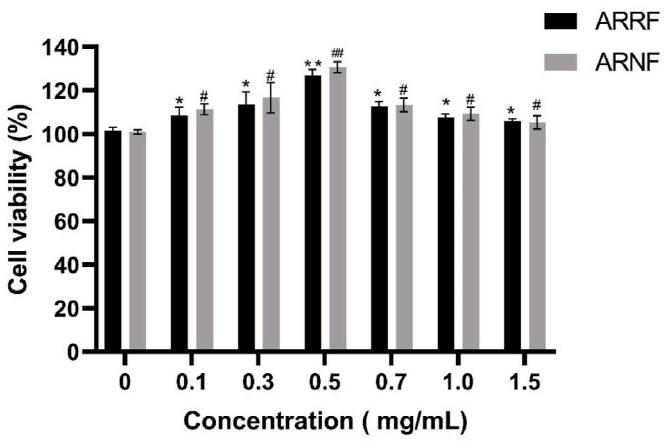

Fig. 10. Effect of peptides ARRF and ARNF on RAW264.7 cell viability. Note: Results are presented as mean ± SD. (n = 3) * indicates a significant difference in ARRF compared with the blank group ($p < 0.05$), ** indicates an extremely significant difference in ARRF compared with the blank group ($p < 0.01$); # indicates that ARNF is significantly different from the blank group at $p < 0.05$, and ## indicates that ARNF is extremely significantly different from the blank group at $p < 0.01$.

between 4.5 and 10.5 Å (Fig. 9A). The RMSF of the ligand ranged from 3.0 to 48.0 Å (Fig. 9C), and the RMSF results for the TLR4 protein with ARRF are shown in Fig. 9B, with the total RMSF value of the protein below 3.4 Å. During the simulation of TLR4 and ARRF, Glu254, Leu283, Glu286, Cys306, and Ser311 were critical in forming hydrogen bonds with ARRF. His257 exhibited hydrophobic interactions during the simulation, while residue Ser311 also displayed ionic interactions (Fig. 9D).

3.6. Effect of peptides ARRF and ARNF on the viability of Raw264.7 cells

To establish the non-toxic concentration range of peptides ARRF and ARNF, the effects of varying concentrations of these peptides on RAW264.7 cell viability were assessed using the CCK-8 assay. Fig. 10 demonstrates that, compared to the control group (0 μg/mL), the survival rates of peptides ARRF and ARNF in the concentration range of 0.1–1.5 mg/mL exceed 100%, indicating the absence of cytotoxicity for these peptides within this range. However, cell proliferation rates decreased when the peptides ARRF and ARNF exceeded 0.5 mg/mL; thus, a concentration of 0.5 mg/mL was selected for subsequent experiments.

3.7. The morphological characteristics of RAW264.7 cells and the effects of peptides ARRF and ARNF on the secretion of NO, TNF-α, IL-6, and PGE_2 were examined

Under treatment with peptides ARRF and ARNF, the morphology of Raw264.7 cells is depicted in Fig. 11A. The cells in the control group, specifically normal Raw264.7 cells, were round, whereas the cells in the model group following LPS stimulation exhibited a spindle or elongated spindle morphology. Furthermore, the quantity of spindle or elongated spindle-shaped cells decreased following treatment with peptides ARRF and ARNF. These results indicate that peptides ARRF and ARNF may alleviate inflammation by inhibiting the differentiation of Raw264.7 cells. The effect of peptides ARRF and ARNF on the secretion of NO by Raw264.7 cells is illustrated in Fig. 11B. In normal Raw264.7 cells, the expression of NO is minimal. Following LPS stimulation, the cells in the model group secrete a substantial amount of NO. The concentration of NO significantly decreased following treatment with peptides ARRF and ARNF ($P < 0.01$). Under LPS induction, Raw264.7 cells can release or upregulate various inflammatory mediators, including TNF-α, IL-6, and IL-1β. The effects of peptides ARRF and ARNF on the secretion of TNF-α, IL-6, and PGE2 by Raw264.7 cells are illustrated in Fig. 11C–E. Compared to the blank group, the levels of TNF-α, IL-6, and PGE2 in the supernatant of LPS-stimulated RAW264.7 cells were significantly increased ($P < 0.01$). In comparison to the model group, peptides ARRF and ARNF significantly reduced the levels of TNF-α, IL-6, and PGE2 in the supernatant of Raw264.7 cells ($P < 0.01$). These results indicate that peptides ARRF and ARNF can inhibit the secretion of TNF-α, IL-6, and PGE2 by Raw264.7 cells, thereby alleviating the inflammatory response.

3.8. Effects of peptides ARRF and ARNF on ROS content, SOD, MDA, and GSH-Px levels in RAW264.7 cells

When stimulated by LPS, RAW264.7 cells produce oxidative stress. ROS serve as critical mediators in the development of oxidative stress. In this experiment, the DCHF-DA fluorescent probe method was employed

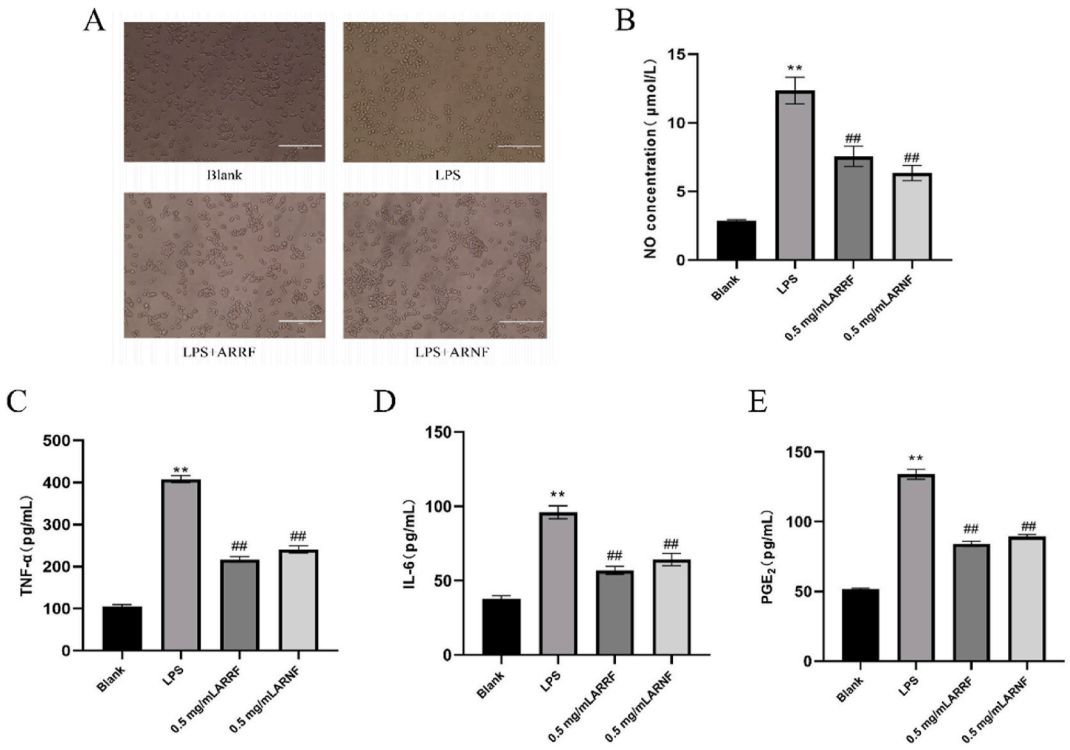

Fig. 11. The effects of polypeptides ARRF and ARNF on the morphology(10A), NO secretion(10B), TNF-α(10C), IL-6(10D), and PGE_2(10E) contents of RAW264.7 cells induced by LPS were studied Note: Results are presented as mean ± SD. (n = 3) ** indicates that the difference is extremely significant compared with the blank group($P < 0.01$); ## indicates extremely significant difference compared with LPS induced group($P < 0.01$).

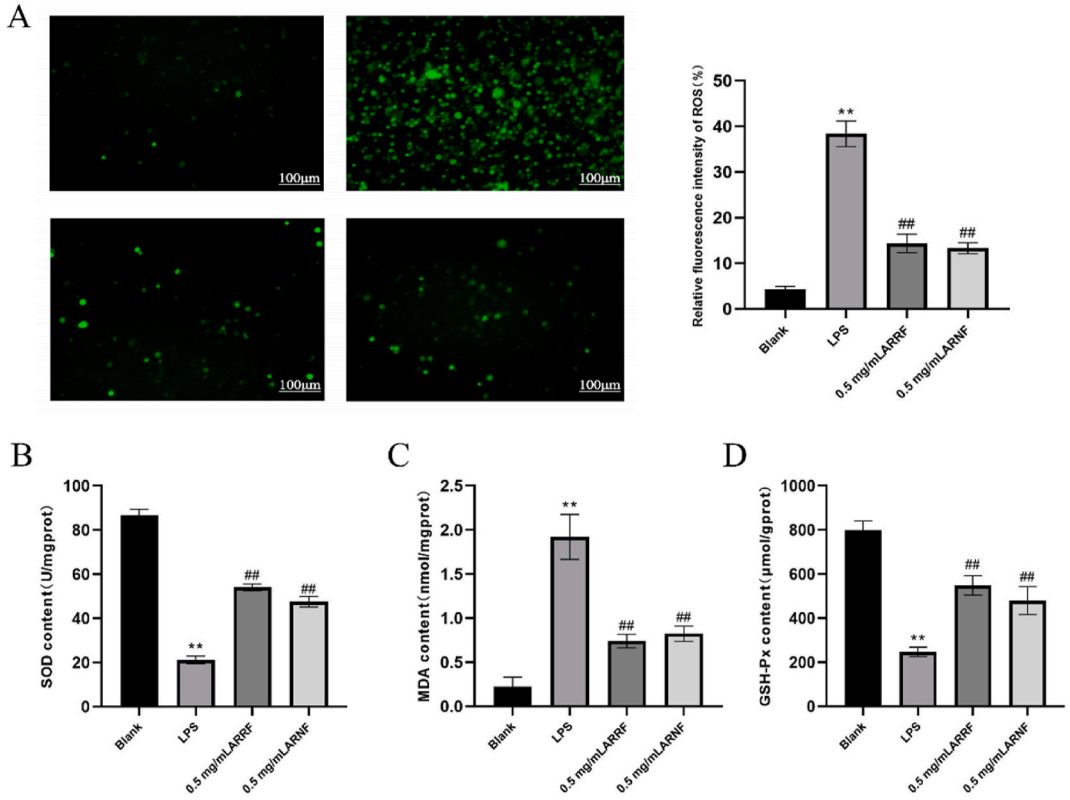

Fig. 12. Effect of peptides ARRF and ARNF on intracellular ROS (11A), SOD (11B), MDA (11C) GSH-Px in RAW264.7 cells induced by LPS Note: Results are presented as mean ± SD. (n = 3) ** indicates that the difference is extremely significant compared with the blank group($P < 0.01$); ## indicates extremely significant difference compared with LPS induced group($P < 0.01$).

to detect the relative levels of intracellular ROS, as illustrated in Fig. 12A. Compared to the LPS group, peptides ARRF and ARNF significantly reduced the relative levels of intracellular ROS induced by LPS ($P < 0.01$). In comparison to the LPS group, peptides ARRF and ARNF significantly increased the activities of SOD and GSH-Px ($P < 0.01$). As illustrated in Fig. 12C, compared to the control group, the LPS group significantly stimulated the production of MDA in cells ($P < 0.01$), and moreover, peptides ARRF and ARNF significantly inhibited the production of MDA ($P < 0.01$). These findings suggest that peptides ARRF and ARNF possess enhanced antioxidant capacity.

CRediT authorship contribution statement

Xuan-Ying Xin: Conceptualization, Data curation, Methodology, Software, Writing – original draft. **Chao-Hui Ruan:** Data curation, Investigation. **Yi-Hui Liu:** Conceptualization. **Huai-Na Jin:** Conceptualization, Formal analysis, Software. **Sung-Kwon Park:** Conceptualization, Formal analysis, Validation, Writing – review & editing. **Sun-Jin Hur:** Conceptualization, Software, Writing – review & editing. **Xiang-Zi Li:** Validation, Writing – review & editing. **Seong-Ho Choi:** Methodology, Validation, Writing – review & editing.

4. Discussion and conclusions

In this study, we used a combination of virtual enzymatic hydrolysis, molecular docking, and molecular dynamics simulations to screen several potential peptides derived from bovine hemoglobin with antioxidant and anti-inflammatory activities. Firstly, using virtual enzymatic hydrolysis, we simulated the effects of various digestive enzymes on bovine hemoglobin, identifying numerous potential bioactive peptides. Concurrently, water solubility, toxicity, and sensitization are crucial indicators for evaluating the metabolism, transport, and distribution of compounds in the body. The prerequisite for the biological activity of bioactive peptides is that they must be non-toxic; therefore, we conducted predictive analyses of their biological activity, toxicity, water solubility, and sensitization. Finally, nine oligopeptides, including DSF, KGTF, ARNF, QADF, DKF, ERMF, RRF, ARRF, and VYFR, were screened. We compared these nine oligopeptides with known bioactive peptides in the BIOPEP database and found that none had been previously reported. BIOPEP is the most comprehensive and up-to-date database of bioactive peptides. To date, the BIOPEP database has recorded 5000 peptides with known functional activities. Further analysis of these nine oligopeptides revealed that all contained the hydrophobic amino acid phenylalanine (Phe). Studies have shown that the activity of antioxidant peptides is related to their amino acid composition, sequence, structure, and metal ion complexation. Antioxidant peptides are generally composed of fewer than 20 amino acid residues, and their antioxidant capacity is enhanced when the terminal ends contain hydrophobic amino acids such as phenylalanine, alanine, leucine, and valine (Vargas-Bello-Pérez et al., 2019). GUHA et al. (Guha and Majumder, 2019) demonstrated that the sequences of most anti-inflammatory peptides are rich in positively charged hydrophobic amino acids, particularly when these amino acids are present at the N or C termini, which are considered critical for anti-inflammatory responses. Our results indicate that nine peptides selected through virtual enzymatic hydrolysis and molecular simulation comprise fewer than 20 amino acids, all of which contain the hydrophobic amino acid phenylalanine (Phe). This finding corroborates previous studies indicating that antioxidant peptides typically consist of fewer than 20 amino acid residues. When the terminal of a peptide contains hydrophobic amino acids, such as phenylalanine, alanine, leucine, and valine, the antioxidant capacity is enhanced. Additionally, the sequences of these nine peptides are rich in positively charged hydrophobic amino acids. Previous studies have shown that the sequences of most anti-inflammatory peptides also exhibit a high abundance of positively charged hydrophobic amino acids, particularly when these amino acids are located at the N or C termini, which are critical for anti-inflammatory responses. Therefore, we speculated that these nine oligopeptides may exhibit superior antioxidant and anti-inflammatory effects. Molecular docking is a widely used computational method to simulate molecular interactions and predict their binding modes and affinities. It is frequently employed in studying the activity of bioactive peptides. Lower binding energy between molecules indicates better affinity between peptides and proteins, theoretically leading to stronger antioxidant and anti-inflammatory activities (Pinzi and Rastelli, 2019). Studies have demonstrated that the Keap1-Nrf2 pathway is a key mechanism for eliminating oxidative stress *in vivo*. In the Keap1-Nrf2 pathway, Nrf2 factors bind to the antioxidant response element (ARE) sequence after nuclear translocation, initiating the expression of heme oxygenase-1 and thereby activating the defense system against oxidative stress. Under oxidative stress, exogenous antioxidants disrupt the Keap1-Nrf2 interaction, ultimately activating the ARE sequence and regulating the expression of various antioxidant enzymes (e.g., catalase, superoxide dismutase, and glutathione peroxidase) in cells, thus enhancing the body's antioxidant capacity (Liu et al., 2022). To further screen bovine hemoglobin-derived antioxidant peptides and elucidate their molecular mechanisms within the Keap1-Nrf2 pathway, molecular docking analysis was conducted between the oligopeptides and the Keap1 receptor. The results indicated that the oligopeptides exhibited strong binding affinity with the Keap1 receptor, successfully penetrating the deeper regions of the protein binding site. The primary binding sites were Val465, Thr560, Gly464, Val604, and Gly605, with Val465 being the most frequently involved. This suggests that the oligopeptide binds to Keap1 mainly through hydrogen bonds or hydrophobic interactions, thereby inhibiting Keap1, while activating Nrf2, thereby reducing the level of oxidative stress.

Keap1 serves as a negative regulator of Nrf2 and plays a pivotal role in maintaining cellular REDOX balance. When Keap1 binds to Nrf2, it inhibits Nrf2 activity, thereby suppressing the expression of antioxidant genes. Our results demonstrated that these nine peptides could bind to Keap1 and prevent its interaction with Nrf2, leading to Nrf2 activation and increased expression of antioxidant genes, thereby enhancing cellular antioxidant capacity. This interaction resembles the mechanism of action of known antioxidants, which typically reduce oxidative stress by enhancing the expression or activity of antioxidant enzymes.

As a receptor primarily recognizing LPS, TLR4 plays a critical role in the inflammatory response. Upon recognizing LPS, TLR4 activates the downstream NF-κB signaling pathway, inducing the production of inflammatory factors associated with endothelial cells (Pei et al., 2010). The results indicated that the oligopeptides exhibited strong binding affinity with the TLR4 receptor, with primary active binding sites being Asn309, Asn305, Glu286, Cys281, Glu254, and Leu283; notably, Asn309 was the most frequently involved at the TLR4 docking site. These results suggest that oligopeptides primarily interact with TLR4 through hydrogen bonding and hydrophobic interactions, thereby exerting anti-inflammatory activity. Molecular dynamics simulations were conducted to evaluate the interactions between these oligopeptides and the Keap1 and TLR4 receptors. Our results demonstrated that the complexes formed by the binding of these bioactive peptides to the Keap1 and TLR4 receptors exhibited distinct kinetic characteristics during the simulation. Specifically, the QADF/Keap1 and RRF/TLR4 complexes attained equilibrium after 10 ns and 30 ns, respectively, which time scales correspond with the findings of the study by ZU et al. (Zu et al., 2024). However, it is important to note that the rate at which they achieved equilibrium may be influenced by various factors, including peptide structure, receptor conformational changes, and simulation conditions. Further analysis revealed that the average RMSD values for QADF/Keap1 and RRF/TLR4 were 1.08 and 2.36 Å, respectively; these values were lower than those of the other complexes, indicating that QADF/Keap1 and RRF/TLR4 exhibit greater stability during the simulation. Our results further underscore the distinctive stability of these specific peptides upon binding to the Keap1 and TLR4

receptors. Additionally, we found that the two peptides, ARRF and ARNF, were capable of stably binding to the Keap1 and TLR4 receptors, suggesting that they may exhibit multifunctional activities. This finding provides new insights into the potential applications of these peptides within the food industry and public health. Notably, these bioactive peptides exhibit low RMSF values, below 1.2 Å for most sequences associated with Keap1 receptor proteins and below 2 Å for most sequences associated with TLR4, which further supports their stability upon receptor binding. Our study not only confirms the binding capacity of these bioactive peptides to the Keap1 and TLR4 receptors, but also offers insights into their binding stability and kinetic characteristics through kinetic simulations. These findings serve as a valuable reference for future studies and may promote the application of these peptides across a broader range of fields. Additionally, we found that the RMSF of these bioactive peptides was low, with most sequences on the Keap1 receptor protein below 1.2 Å and most sequences on TLR4 below 2 Å. This suggests that these two protein systems were relatively stable, consistent with the molecular docking results. Our results demonstrate that these peptides not only bind to antioxidant and anti-inflammatory target proteins but also exhibit high stability in molecular dynamics simulations, laying the foundation for their application in functional food and drug development. TLR4 is a crucial immune receptor that recognizes various pathogen-associated molecular patterns and damage-associated molecular patterns to initiate innate immune responses. These nine peptides were shown to bind to TLR4 and modulate its activity through molecular simulation technology, indicating that these peptides possess immunomodulatory functions that can influence the direction and intensity of inflammatory or immune responses. This interaction may resemble the mechanism of action of known anti-inflammatory peptides, which typically exert their effects by inhibiting the release of inflammatory mediators or modulating immune cell function.

In the experimental verification, we thoroughly evaluated the anti-inflammatory and antioxidant effects of peptides, selecting two oligopeptides, ARRF and ARNF, for cellular experiments to validate the accuracy of virtual enzymatic hydrolysis and molecular simulation. LPS-stimulated RAW264.7 cells were utilized to induce inflammation and oxidative stress, representing the host immune defense response against foreign pathogens. The body recognizes pathogen-associated molecular patterns of various invading microorganisms, including flagellin and LPS, through pattern recognition receptors on the surface of antigen-presenting cells, such as macrophages. Upon stimulation by LPS, a significant amount of ROS is produced (Guo et al., 2024). The results of this study demonstrated that peptides ARRF and ARNF could inhibit intracellular MDA content and relative ROS levels induced by LPS, enhance the activity of antioxidant enzymes, and thus confer protective effects against LPS-induced oxidative stress in RAW264.7 cells. Furthermore, oxidative stress is closely associated with inflammation. ROS produced by LPS stimulation can activate the NF-κB signaling pathway, a key signaling pathway in inflammation, promoting the expression of TNF-α, IL-6, and other inflammatory factors. NO is also a key signaling molecule involved in oxidative stress and inflammatory responses. In this study, peptides ARRF and ARNF also reduced LPS-induced secretion of pro-inflammatory cytokines and NO release, thereby exerting anti-inflammatory effects. These findings are consistent with the results of molecular simulations, indicating that utilizing virtual enzymatic hydrolysis and molecular simulations is a feasible approach for screening bioactive peptides. However, due to the extensive diversity of bioactive peptides, verifying all such peptides is challenging. Consequently, this study verified two multifunctional peptides, although certain limitations remain. This study aims to further elucidate the significance of molecular mimicry in the field of foodborne bioactive peptides.

In this study, we investigated the anti-inflammatory and antioxidative effects of bioactive peptides derived from bovine hemoglobin through virtual enzymatic digestion and molecular simulation; the accuracy of this molecular simulation technology was validated through experimental confirmation. Although this study specifically focused on bovine hemoglobin, the employed methodology is broadly applicable to proteins from various sources. Other protein sources may also serve as excellent candidates for peptide extraction. Peptides exhibiting similar or distinct biological activities may be generated from various protein sources, thereby creating significant opportunities for the discovery of novel functional peptides. Furthermore, peptides with potential health benefits may be produced from plant proteins using a similar approach, thus broadening the applicability of this study. These peptides exhibit beneficial biological activities and can be widely utilized in various food products, particularly through the preparation of bovine hemoglobin peptides in the future. For instance, they may be utilized as natural antioxidants to prolong the shelf life of food products or as functional additives to enhance nutritional value. Additionally, these peptides possess considerable market potential. Bioactive peptides can be formulated into capsules, tablets, or liquid supplements to support specific health objectives, such as enhancing immune function, promoting muscle growth, or improving cardiovascular health. Given their natural origin and potential multiple health benefits, these peptide supplements are anticipated to gain widespread consumer acceptance.

In summary, this study identified peptides with potential anti-inflammatory and antioxidant activities through virtual enzymatic digestion and activity prediction, followed by docking the target peptides with Keap1 and TLR4 using molecular docking and molecular dynamics simulations. Finally, QADF was identified as an excellent antioxidant peptide derived from bovine hemoglobin, while RRF was identified as an excellent anti-inflammatory peptide derived from bovine hemoglobin. ARRF and ARNF were identified as multifunctional peptides with both antioxidant and anti-inflammatory activities. Cell experiments demonstrated that ARRF and ARNF effectively ameliorated LPS-induced oxidative stress and inflammation in RAW264.7 cells. Compared to traditional methods of separation, purification, and identification following enzymatic hydrolysis, this approach allows for the rapid and efficient screening of bovine hemoglobin peptides with antioxidant and anti-inflammatory activities, offering a novel strategy for the rapid screening of bioactive peptides. Despite thorough screening and evaluation using biological activity prediction and molecular simulation techniques, limitations may still exist, including the potential that not all peptides were fully considered for their biological activities. In the future, we will conduct more in-depth research on it.

Data statement

The data that support the findings of this study are available from the corresponding author upon reasonable request.

Funding

This study was supported by the National Natural Science Foundation of China (grant number: 32060767) and the Research Fund of Engineering Research Center of North-East Cold Region Beef Cattle Science & Technology Innovation, Ministry of Education, and the “111” Project (D20034), China.

Declaration of competing interest

All authors disclosed no relevant relationships!

Data availability

Data will be made available on request.

References

Abou-Diab, M., Thibodeau, J., Deracinois, B., et al., 2020. Bovine hemoglobin enzymatic hydrolysis by a new eco-efficient process-Part II: production of bioactive peptides. Membranes 10 (10), 268. https://doi.org/10.3390/membranes10100268. Published 2020 Sep. 29.

Amer, S.A., Farahat, M., Khamis, T., et al., 2022. Evaluation of spray-dried bovine hemoglobin powder as a dietary animal protein source in nile Tilapia, Oreochromis niloticus. Animals (Basel). 12 (22), 3206. https://doi.org/10.3390/ani12223206. Published 2022 Nov 18.

Arulselvan, P., Fard, M.T., Tan, W.S., et al., 2016. Role of antioxidants and natural products in inflammation. Oxid. Med. Cell. Longev. 2016, 5276130. https://doi.org/10.1155/2016/5276130.

Aung, S.H., Abeyrathne, E.D.N.S., Ali, M., Ahn, D.U., Choi, Y.S., Nam, K.C., 2023. Comparison of functional properties of blood plasma collected from black goat and hanwoo cattle. Food Sci Anim Resour 43 (1), 46–60. https://doi.org/10.5851/kosfa.2022.e57.

Bellezza, I., Giambanco, I., Minelli, A., Donato, R., 2018. Nrf2-Keap1 signaling in oxidative and reductive stress. Biochim. Biophys. Acta Mol. Cell Res. 1865 (5), 721–733. https://doi.org/10.1016/j.bbamcr.2018.02.010.

Biji, C.A., Balde, A., Nazeer, R.A., 2024. Anti-inflammatory peptide therapeutics and the role of sulphur containing amino acids (cysteine and methionine) in inflammation suppression: a review. Inflamm. Res. 73 (7), 1203–1221. https://doi.org/10.1007/s00011-024-01893-6.

Ciesielska, A., Matyjek, M., Kwiatkowska, K., 2021. TLR4 and CD14 trafficking and its influence on LPS-induced pro-inflammatory signaling. Cell. Mol. Life Sci. 78 (4), 1233–1261. https://doi.org/10.1007/s00018-020-03656-y.

Filomeni, G., De Zio, D., Cecconi, F., 2015. Oxidative stress and autophagy: the clash between damage and metabolic needs. Cell Death Differ. 22 (3), 377–388. https://doi.org/10.1038/cdd.2014.150.

Gao, J., Guo, K., Du, M., Mao, X., 2022. Bovine α-lactalbumin-derived peptides attenuate TNF-α-induced insulin resistance and inflammation in 3T3-L1 adipocytes through inhibiting JNK and NF-κB signaling. Food Funct. 13 (4), 2323–2335. https://doi.org/10.1039/d1fo01217g. Published 2022 Feb 21.

Guha, S., Majumder, K., 2019. Structural-features of food-derived bioactive peptides with anti-inflammatory activity: a brief review. J. Food Biochem. 43 (1), e12531. https://doi.org/10.1111/jfbc.12531.

Guo, Y., Zheng, Z., Zhang, G., Zhong, J., Fan, X., Li, C., Zhu, S., Cao, R., Fu, K., 2024. Berberine inhibits LPS-induced epithelial-mesenchymal transformation by activating the Nrf2 signalling pathway in bovine endometrial epithelial cells. Int. Immunopharm. 143 (Pt 1), 113346. https://doi.org/10.1016/j.intimp.2024.113346.

Gupta, S., Kapoor, P., Chaudhary, K., et al., 2013. In silico approach for predicting toxicity of peptides and proteins. PLoS One 8 (9), e73957. https://doi.org/10.1371/journal.pone.0073957. Published 2013 Sep. 13.

Hedhili, K., Dimitrov, K., Vauchel, P., et al., 2015. Valorization of cruor slaughterhouse by-product by enzymatic hydrolysis for the production of antibacterial peptides: focus on α 1-32 family peptides mechanism and kinetics modeling. Bioproc. Biosyst. Eng. 38 (10), 1867–1877. https://doi.org/10.1007/s00449-015-1427-2.

Huang, M.H., Lin, Y.H., Lyu, P.C., et al., 2021. Imperatorin interferes with LPS binding to the TLR4 Co-receptor and activates the Nrf2 antioxidative pathway in RAW264.7 murine macrophage cells. Antioxidants 10 (3), 362. https://doi.org/10.3390/antiox10030362. Published 2021 Feb 27.

Liu, S., Pi, J., Zhang, Q., 2022. Signal amplification in the KEAP1-NRF2-ARE antioxidant response pathway. Redox Biol. 54, 102389. https://doi.org/10.1016/j.redox.2022.102389.

Maurer-Stroh, S., Krutz, N.L., Kern, P.S., et al., 2019. AllerCatPro-prediction of protein allergenicity potential from the protein sequence. Bioinformatics 35 (17), 3020–3027. https://doi.org/10.1093/bioinformatics/btz029.

Minkiewicz, P., Iwaniak, A., Darewicz, M., 2019. BIOPEP-UWM database of bioactive peptides: current opportunities. Int. J. Mol. Sci. 20 (23), 5978. https://doi.org/10.3390/ijms20235978. Published 2019 Nov 27.

Mooney, C., Haslam, N.J., Pollastri, G., Shields, D.C., 2012. Towards the improved discovery and design of functional peptides: common features of diverse classes permit generalized prediction of bioactivity. PLoS One 7 (10), e45012. https://doi.org/10.1371/journal.pone.0045012.

Osman, E.Y., Abdelghafar, H.I., Elsisi, A.E., 2024. TLR4 inhibitors through inhibiting (MYD88-TRIF) pathway, protect against experimentally-induced intestinal (I/R) injury. Int. Immunopharm. 136, 112421. https://doi.org/10.1016/j.intimp.2024.112421.

Outman, A., Deracinois, B., Flahaut, C., et al., 2023. Comparison of the bioactive properties of human and bovine hemoglobin hydrolysates obtained by enzymatic hydrolysis: antimicrobial and antioxidant potential of the active peptide α137-141. Int. J. Mol. Sci. 24 (17), 13055. https://doi.org/10.3390/ijms241713055. Published 2023 Aug 22.

Pei, Z., Li, H., Guo, Y., Jin, Y., Lin, D., 2010. Sodium selenite inhibits the expression of VEGF, TGFbeta(1) and IL-6 induced by LPS in human PC3 cells via TLR4-NF-(K)B signaling blockage. Int. Immunopharm. 10 (1), 50–56. https://doi.org/10.1016/j.intimp.2009.09.020.

Pinzi, L., Rastelli, G., 2019. Molecular docking: shifting paradigms in drug discovery. Int. J. Mol. Sci. 20 (18), 4331. https://doi.org/10.3390/ijms20184331. Published 2019 Sep. 4.

Płóciennikowska, A., Hromada-Judycka, A., Borzęcka, K., Kwiatkowska, K., 2015. Co-operation of TLR4 and raft proteins in LPS-induced pro-inflammatory signaling. Cell. Mol. Life Sci. 72 (3), 557–581. https://doi.org/10.1007/s00018-014-1762-5.

Ranneh, Y., Ali, F., Akim, A.M., et al., 2017. Crosstalk between reactive oxygen species and pro-inflammatory markers in developing various chronic diseases: a review. Appl Biol Chem 60, 327–338. https://doi.org/10.1007/s13765-017-0285-9.

Shaikhaliev, A.I., Krasnov, M.S., Vakhrushev, I.V., et al., 2019. Effect of bioactive peptide complex isolated from bovine serum on proliferation and migration of mesenchymal stromal cells *in vitro* and reparation of bone defects *in vivo*. Bull. Exp. Biol. Med. 168 (1), 178–185. https://doi.org/10.1007/s10517-019-04671-1.

Shuli, Z., Linlin, L., Li, G., et al., 2022. Bioinformatics and computer simulation approaches to the discovery and analysis of bioactive peptides. Curr. Pharmaceut. Biotechnol. 23 (13), 1541–1555. https://doi.org/10.2174/1389201023666220106161016.

Sies, H., Jones, D.P., 2020. Reactive oxygen species (ROS) as pleiotropic physiological signalling agents. Nat. Rev. Mol. Cell Biol. 21, 363–383. https://doi.org/10.1038/s41580-020-0230-3.

Vargas-Bello-Pérez, E., Márquez-Hernández, R.I., Hernández-Castellano, L.E., 2019. Bioactive peptides from milk: animal determinants and their implications in human health. J. Dairy Res. 86 (2), 136–144. https://doi.org/10.1017/S0022029919000384.

Wang, Y., Zhang, T., Zhang, H., Yang, H., Li, Y., Jiang, Y., 2017. Bovine hemoglobin derived peptide asn-phe-gly-lys inhibits pancreatic cancer cells metastasis by targeting secreted Hsp90α. J. Food Sci. 82 (12), 3005–3012. https://doi.org/10.1111/1750-3841.13962.

Yan, D., Chen, D., Shen, J., Xiao, G., van Wijnen, A.J., Im, H.J., 2013. Bovine lactoferricin is anti-inflammatory and anti-catabolic in human articular cartilage and synovium. J. Cell. Physiol. 228 (2), 447–456. https://doi.org/10.1002/jcp.24151.

Yu, C., Xiao, J.H., 2021. The keap1-Nrf2 system: a mediator between oxidative stress and aging. Oxid. Med. Cell. Longev. 2021, 6635460. https://doi.org/10.1155/2021/6635460. Published 2021 Apr 19.

Zu, X., Zhao, Q., Liu, W., Guo, L., Liao, T., Cai, J., Li, H., 2024. Sturgeon (Acipenser schrenckii) spinal cord peptides: antioxidative and acetylcholinesterase inhibitory efficacy and mechanisms. Food Chem. 461, 140834. https://doi.org/10.1016/j.foodchem.2024.140834.